Site occupancy of chlorine on Cu(111) using normal-incidence x-ray standing waves: The energy difference between fcc and hcp hollow sites

A. G. Shard*
Department of Engineering Materials, Sir Robert Hadfield Building, University of Sheffield, Mappin Street, Sheffield S1 3JD, United Kingdom

C. Ton-That
Nanoscience Centre, University of Cambridge, 11 JJ Thomson Avenue, Cambridge CB3 0FF, United Kingdom

P. A. Campbell
School of Physics and Astronomy, St Andrews University, North Haugh, St Andrews, Fife KY16 9SS., United Kingdom

V. R. Dhanak
SRS Daresbury Laboratory and Physics Department, University of Liverpool, Warrington WA4 4AD, United Kingdom
(Received 21 August 2003; revised manuscript received 21 April 2004; published 26 October 2004)

It has previously been established that the lowest energy site for chlorine atoms on Cu(111) is the "fcc" hollow. However, substantial population of the "hcp" hollow at room temperature indicates that there is a relatively small difference in energy between the two sites. We show that this energy difference must be less than 10 meV by measuring the relative populations using normal-incidence x-ray standing waves and comparing the results to Monte Carlo simulations. This result is consistent with recent density functional theory calculations which indicate an energy difference of approximately 5 meV.

DOI: 10.1103/PhysRevB.70.155409 PACS number(s): 68.47.De, 68.49.Uv, 68.43.−h

INTRODUCTION

Most simple surfaces have well-defined sites which represent the minimum energy position for adsorbate atoms. The position of such a site is usually amenable to experimental determination. Complexities arise when there are a number of different adsorption sites of similar energies which are thermally populated by adsorbate atoms. The relative population of each site is influenced by the temperature and the magnitude of energy differences between the sites. Knowledge of the size of these energy differences is essential to a full understanding of the system. Unfortunately, most structural studies concentrate upon ordered phases in which a determination of such energy differences is impossible. In ordered adlayers lateral interactions between adsorbate atoms are at least as important as adsorbate–substrate interactions in determining the populations of different sites. Therefore, one cannot deduce site energy differences by studying the site occupation of ordered phases alone and one must obtain additional information from disordered phases and from phase diagrams.

To derive site energy differences from relative populations it is necessary first to ensure that the system being investigated is at equilibrium and second to use an experimental technique that is able to quantitatively distinguish between adsorption at the various binding sites. The results must then be interpreted using simulations, since obtaining analytical solutions for site population in terms of interaction energies is generally not possible. X-ray standing wave (XSW) techniques are an excellent choice for such studies since they provide, with few assumptions, quantitative registry information for adsorbate atoms irrespective of order in the adsorbed over-layer.[1] This avoids a potential problem of using diffraction techniques, such as low-energy electron diffraction (LEED), in which ordered regions may dominate the data. In a series of experiments[2–4] Schwennicke *et al.* and Schwennicke and Pfnur investigated the lateral interactions of O/Ni(111), using diffuse LEED results and the system phase diagram, demonstrating that both could be modeled using a Monte Carlo simulation and finding an energy difference of 46 meV between the "hcp" and "fcc" hollow sites.

Kadodwala *et al.* investigated the simultaneous adsorption of chlorine and bromine on Cu(111).[5] While the main thrust of their investigation was a demonstration of the versatility of normal incidence XSW (NIXSW), a site energy difference between "fcc" and "hcp" hollows of 13.5 ± 5 meV was also calculated. Although details of the calculation were not provided, this result is consistent with the two level partition function given in Eq. (1) in which N_x is the number of atoms in site x and ε is the energy difference between the two sites.

$$\frac{N_{\mathrm{hcp}}}{N_{\mathrm{fcc}}} = \exp\left(-\varepsilon/kT\right). \tag{1}$$

Use of this equation relies on the assumption that the number of available "hcp" sites is always equal to the number of available "fcc" sites. It is reasonable to suppose that adsorption at a site will preclude another atom adsorbing at the same site. If one considers only the limitation of one adsorbed atom per site, the correct expression can be easily derived and is given in Eq. (2) where theta is fractional coverage following the standard definition (note that a fractional coverage of 2 is obtained when all hollow sites are occupied).

$$\frac{N_{\mathrm{hcp}}}{N_{\mathrm{fcc}}} = \sqrt{z^2 + \exp\left(-\varepsilon/kT\right)} - z;$$

$$z = \frac{(1-\theta)\left[1-\exp\left(-\varepsilon/kT\right)\right]}{2}. \quad (2)$$

Even this expression is not appropriate for halogen atoms on Cu(111) since lateral interactions between atoms in nearby sites must also be taken into account. There are additional difficulties in using the experimental population ratios found by Kadodwala[5] to calculate energy differences. The measurements were performed at a low temperature (130 K) and equilibrium may not be achieved on the timescale of the experiment. In this work we demonstrate that, even at higher temperatures (180 K), equilibrium in the Cl/Cu(111) system is not attained on a timescale of hours and this observation invalidates any calculation in which equilibrium is assumed. Since lateral interactions in the mixed chlorine/bromine system are intrinsically more complicated than the single adsorbate alternative, then this study of a mixed system is clearly not ideal.

In an XSW experiment an appropriate geometry and x-ray energy is used to establish a Bragg reflection from the single crystal substrate. The incoming and outgoing photons interfere to produce a standing wavefield of x-ray intensity with the same periodicity as and parallel to the scattering planes. The nodes of the wave field move relative to the scattering planes as either the angle of the crystal, or the photon energy, is scanned through the Bragg condition. By monitoring the photoemission intensity of atoms during this scan it is possible to establish their height normal to the nearest bulk scattering plane (or extension thereof beyond the bulk of the crystal).[1] Analysis of the intensity profiles returns two parameters, the coherent position (P) and coherent fraction (F), which can be interpreted, respectively, as the height of the atomic species above the nearest extended plane and the fraction of atoms at that height, assuming the remainder to be distributed in an isotropic manner. When the atoms have a distribution of heights with respect to the scattering plane the expected F,P can be calculated from the height distribution function $f(z)$ using Eq. (3), where z is the height in units of the lattice spacing.

$$F\exp(2\pi iP) = \int f(z)\exp(2\pi iz)dz. \quad (3)$$

In situations where there are discrete sites a summation can be employed, as in Eq. (4). This is essentially a vector sum, which is most easily visualised on an Argand diagram with F (f) as the modulus and P (p) as the argument of a complex number.[6]

$$F\exp(2\pi iP) = \sum_n f_n \exp(2\pi i p_n). \quad (4)$$

The application of NIXSW to study adsorbates on single crystal metal surfaces was described by Woodruff *et al.*[7] At normal incidence the Bragg energy changes minimally with small variations in reflection angle and this permits XSW experiments to be performed on metal crystals, which display a greater degree of mosaicity than, for example, semiconductor crystals. In their seminal work, Woodruff *et al.* used the Cu(111)$-(3\sqrt{3}\times\sqrt{3})$R30°-Cl structure to demonstrate the approach and it is an amenable system to study because of the high C1 K edge cross section at the photon energy used for the $\langle 111\rangle$ reflection (approximately 2975 eV). In this work we employ the same system and find identical results for the $\sqrt{3}$ surface. We extend the previous work to include disordered surfaces and, using NIXSW to quantify the relative populations of hollow sites, find limiting values for the difference in energy between the two sites.

EXPERIMENT

A. NIXSW experiments

Experiments were performed on BL4.2 at the Daresbury SRS,[8] the beamline has a double crystal monochromator which was equipped with Ge(111) crystals. The UHV end chamber was equipped with a VG CLAM2 hemispherical analyser positioned at 50° to the incoming beam, LEED optics and a fluorescent screen positioned around the beam entrance port to assist in aligning the crystal by visualizing the reflected x-rays. The Cu(111) crystal was mounted on a XYZ manipulator with polar and azimuthal rotation and prepared by cycles of argon ion sputtering and annealing to approximately 500°C.

The crystal was deemed to be clean when a sharp (1×1) LEED pattern was observed and electron energy distribution curves (EDCs) showed no evidence of any element apart from copper. Chlorine was generated from an *in situ* solid state electrochemical cell.[9] Chlorine dosing was carried out at room temperature prior to changing the temperature of the sample, with the exception of experiments (which are discussed later) in which dosing was carried out with the crystal cooled by liquid nitrogen. The coverage of chlorine was determined from the intensities of the Cl KLL (2401 eV) and Cu LMM (922 eV) Auger electron peaks in EDCs taken with a photon energy of 2976 eV. Intensity ratios were converted to coverage by using the known coverage of $\theta=1/3$ for the Cu(111)-$(\sqrt{3}\times\sqrt{3})$R30°-Cl structure and assuming that within the range of coverages employed, the Cl/Cu intensity ratio is proportional to fractional coverage.

NIXSW measurements were carried out in a manner described previously.[10] The sample was aligned with either the (111) or (1-11) planes normal to the incident radiation. The position was optimized by monitoring the reflected current in the beamline I_0 beam monitor. The photon energy was then scanned through the Bragg energy over a range of 20 eV in a stepwise fashion. The reflectivity profile was measured from the I_0 monitor and in all cases was symmetrical and Gaussian in shape. At each point the Cl KLL and Cu MNN intensities were measured by subtracting the background counts taken at a kinetic energy 20–30 eV higher than the peaks from the peak counts. These measurements provide the characteristic XSW profiles which can be analyzed to determine the two structural parameters, the coherent fraction, and the coherent position. The total electron yield was measured simulta-

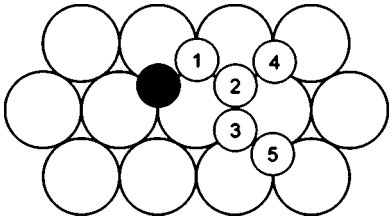

FIG. 1. Pairwise interactions considered during Monte Carlo simulations, up to the fifth nearest neighbour [corresponding to the distance between chlorine atoms in the Cu(111)-($\sqrt{3}\times\sqrt{3}$)R30°-Cl structure]. Note that the van der Waal's diameter of chlorine falls between the third and fourth nearest neighbour distances.

neously to characterize the energy and width of the standing wave which are required for the analysis. The excitation of Cl KLL emission by electrons emitted from the substrate is thought to be negligible in this experiment as there is little emission above the Cl *K*-edge, and these effects are thought to be significant only when the excitation energy for Auger electron emission is low.[11]

B. Monte Carlo simulations

To model the experimental results we employed Monte Carlo simulations using a similar methodology to that of Schwennicke and Pfnur.[4] Monte Carlo simulations were performed on a lattice of 102×102 fcc sites and a similar number of hcp sites using periodic boundary conditions. Atoms in sites on the lattice were randomly selected, and movement to a neighboring site was governed by the energy difference between the two sites. The Metropolis algorithm[12] was employed; if the new site is lower in energy then the atom is moved, if the new site is higher in energy then the atom moves with a probability equal to $\exp(-\Delta E/kT)$. A Mersenne twister random number generator was used,[13] which repeats after (2^{19937}-1) iterations (a typical simulation consisted of $\sim10^{12}$ calls to the generator). Site energies were calculated by a summation of the energy associated with the type of site (hcp or fcc) and pairwise interactions up to the fifth nearest neighbor interaction (e_1 to e_5), see Fig. 1. Thus, the energy of the current site of the atom is calculated and the energy of the new site based on both the identity of the site and the number and distance of nearby atoms. The difference between the two values is ΔE, which is used as described above. The neglect of longer range interactions is justifiable since there is no evidence of ordering on a longer length scale, such as a $p(2\times2)$ superstructure, for example, and we find the results can be adequately modeled with $e_5=0$, as described later. The nearest and next-nearest (e_1 and e_2) interactions were set to be arbitrarily large since these represent distances (1.48 and 2.56 Å) significantly shorter than the van der Waals diameter of chlorine (3.60 Å). The energies chosen were large enough to prevent interatomic distances of these unphysically short values occurring during the simulation. The distance of the third nearest neighbor (e_3) is also shorter than this diameter (2.95 Å), but this interaction must be allowed to permit movement of atoms from a ($\sqrt{3}\times\sqrt{3}$)R30° arrangement. The interaction energies e_3, e_4 (3.91 Å), and e_5 (4.43 Å) were varied relative to the hcp-fcc site energy difference (ε), including attractive potentials for e_5. To be physically realistic we assume that $e_3>e_4>e_5$ and did not carry out simulations in which this order was changed. After many iterations the average value of site occupation converges on an equilibrium value for a given temperature. By changing the temperature in subsequent simulations it is possible to obtain a relationship between temperature and site occupation for any given set of interaction energies and coverages. A wide range of values for e_3, e_4, and e_5 were investigated ranging from 0 to 40ε for e_3, 0 to 20ε for e_4, and -4ε to 4ε for e_5. Coverages ranged from 0.1 to 0.333 ML. The purpose of these simulations is to find the set, or sets of interaction and site energies that best match the experimental data.

Simulations were initially carried out to determine the ($\sqrt{3}\times\sqrt{3}$)R30° and, where appropriate, (2×2) disorder temperatures for each set of parameters. The first temperature calibrates the energy scale, since this disorder temperature is known to be 330 K, the second is a useful check, as the (2×2) structure has not been reported for this system and we did not observe it even while dosing at 190 K.

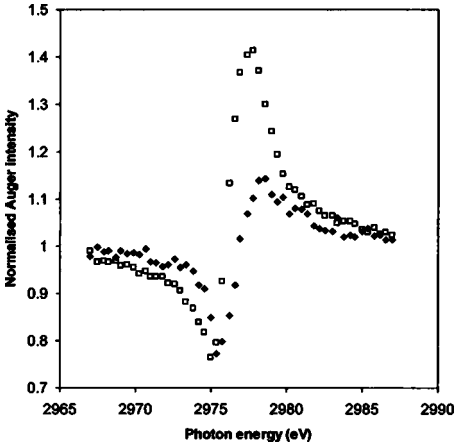

FIG. 2. X-ray standing wave profiles taken at normal incidence to the ⟨111⟩ planes for the Cu(111)-($\sqrt{3}\times\sqrt{3}$)R30°-Cl surface of copper (squares) and chlorine (diamonds). The data were acquired by monitoring the peak height of the Cu LMM and Cl KLL Auger electron peaks, respectively. The difference in the shape of the profiles results from a different position of the atoms relative to the atomic scattering planes of the copper crystal.

RESULTS AND DISCUSSION

A. NIXSW experiments

The NIXSW profiles of copper and chlorine using the ⟨111⟩ reflection are shown in Fig. 2. Analysis of these profiles leads to a coherent position of 0.873 ± 0.02 and coherent fraction of 0.92 ± 0.04 for chlorine, which implies chlorine atoms reside at a height of 1.81 Å above the top layer of copper atoms (or more strictly, above an extension of the bulk scattering planes) with good order. This is entirely in accord with previous results on the same system.[7,14] Estimates of error are based on six independent experiments at a

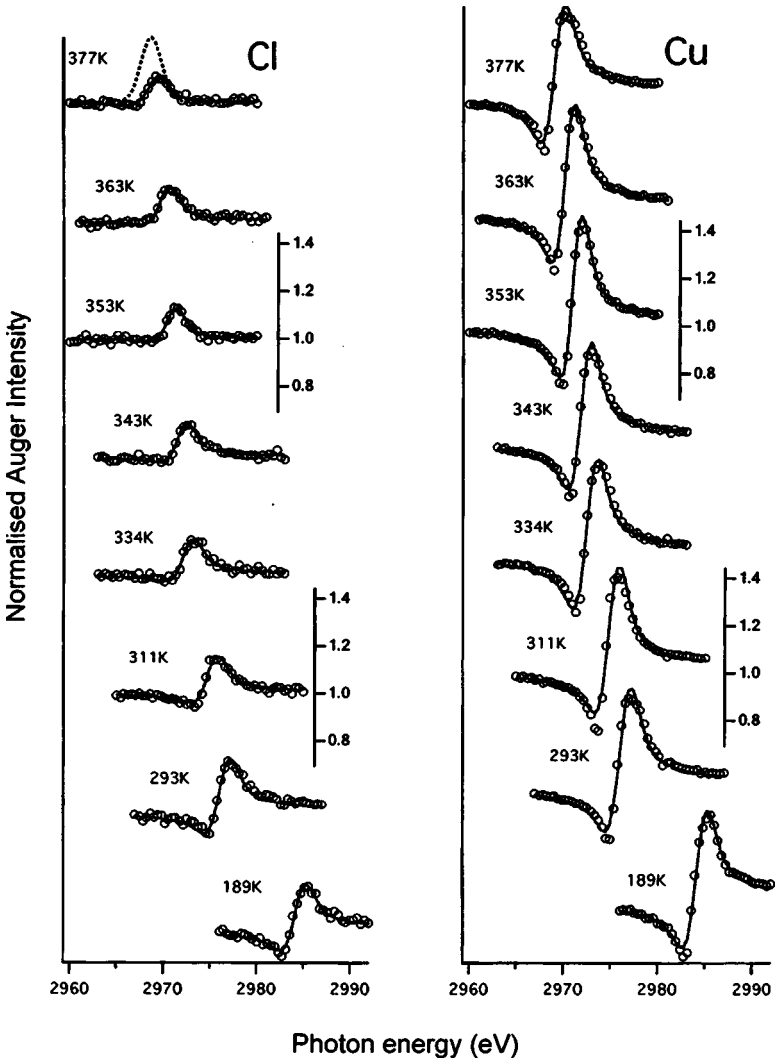

FIG. 3. X-ray standing wave profiles taken at normal incidence to the $\langle 1-11 \rangle$ planes at a variety of different temperatures and one third monolayer coverage with best fits (solid line). All traces have the same normalized Auger intensity scale, but shifted vertically for clarity, scale bars are provided for the 311 and 353 K traces. The Bragg energy changes with the thermal expansivity of copper as expected, but there is no significant change in the copper XSW profile. The disorder transition of the Cu(111)-($\sqrt{3}\times\sqrt{3}$)R30°-Cl structure is evident in the change in the chlorine XSW profile around 330 K. The high temperature, disordered surfaces do not have isotropically distributed chlorine atoms as demonstrated by the expected profile for such a surface (dashed line mapped onto top trace). The trace at 189 K was obtained by dosing chlorine at room temperature and then cooling the crystal, see text.

variety of temperatures and coverages and it was found that there was no systematic variation in $F_{(111)}$ and $P_{(111)}$ with these parameters or with the existence of ordered phases. This result indicates that the height of chlorine atoms is governed by interactions between the copper surface and individual chlorine atoms and is unaffected by lateral interactions between chlorine atoms.

Results of NIXSW experiments from the $\langle 1-11 \rangle$ reflection taken with a fixed coverage of $\theta=0.33$ and at a variety of temperatures are shown in Fig. 3. Below the disorder transition the profile is similar in shape to the copper profile. As the temperature is increased the characteristic "dip" in intensity is lost and the profile becomes more Gaussian in shape, which is the expected profile of an isotropic distribution. However, the peak intensity in these disordered surfaces are less than expected for an isotropic distribution, an example of which is mapped onto the top trace. These results imply that there is still a degree of site ordering in the chlorine atom distributions even when there is no long range order in the overlayer. From the coherent fraction for the $\langle 111 \rangle$ reflection it can be shown that the expected values of $P_{(1-11)}$ are 0.291, 0.624, and 0.958 for the atop, hcp hollow, and fcc hollow sites, respectively. If it is assumed that chlorine atoms occupy only the hollow sites and that there will always be a larger population of atoms in the fcc hollows then it is to be expected that the $P_{(1-11)}$ results will be between 0.791 and 0.958. The results from this reflection for all temperatures and coverages fall between 0.81 and 0.94 which is consistent with expectations and indicates the fraction of atoms in hcp hollow sites varies from approximately 0.46 to 0.10 depending on conditions. Coherent fractions from this reflection at coverages of 0.33 and lower were approximately three quarters of that expected from the $F_{(111)}$ result. This reduction in coherent fraction is probably due to a greater amplitude of lateral thermal motion compared to vertical thermal motion resulting from shallower confining potentials in the lateral directions. Another possibility is a contribution from chlorine atoms adsorbed at defect sites. If such atoms were present in significant numbers, they would only affect our analysis of the results if they were not isotropically distributed with respect to height above the (1-11) planes. We therefore assume that the copper crystal does not have a large number of defect sites or that chlorine atoms adsorbed at defect sites are isotropically distributed with respect to the off-normal reflection plane.

The results are summarized in the Argand diagram given in Fig. 4. Results are plotted with polar coordinates $(F, 2\pi P)$

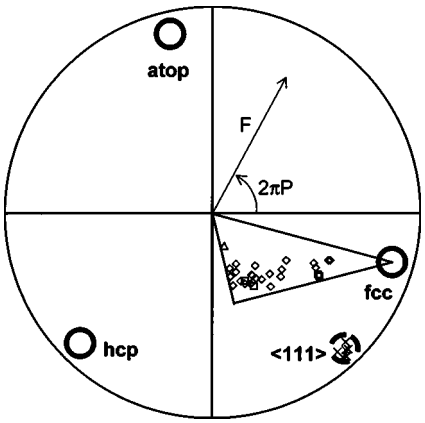

FIG. 4. Argand diagram summary of chlorine NIXSW results, the structural parameters F and P are treated as the modulus and argument of a complex number. The ⟨111⟩ results (crosses) appear in the lower right-hand quadrant, from which the expected positions for the three high symmetry sites in the ⟨1-11⟩ reflection can be calculated (shown by bold circles). If the atoms are only in hollow sites, with the majority in the fcc hollow then ⟨1-11⟩ results are expected to fall within the large right angled triangle. All ⟨1−11⟩ data points comply with this expectation (diamonds) including the Cu(111)-$(6\sqrt{3}\times 6\sqrt{3})$R30°-Cl result (small triangle) and results acquired at 189 K (squares).

and the large triangle represents the expected range of results from the ⟨1−11⟩ reflection based on the ⟨111⟩ results and assuming only fcc and hcp occupation. Using this assumption, the $P_{(1-11)}$ values can be used to calculate the fraction of atoms in hcp hollow sites, as shown in Eq. (5), in which P_{fcc} is the expected coherent position if all atoms were in fcc sites. The derivative of this equation indicates that XSW will be more sensitive (by a factor of approximately 4) to small changes in fractional occupation when both sites are equally occupied than when one site is fully occupied. However, this increase in sensitivity is somewhat offset by an increased error in the determination of coherent position when the coherent fraction is low.

$$f_{\mathrm{hcp}} = \frac{2\,\tan[2\pi(P_{\mathrm{fcc}} - P_{11\bar{1}})]}{3\,\tan[2\pi(P_{\mathrm{fcc}} - P_{11\bar{1}})] + \sqrt{3}}. \qquad (5)$$

We include some results in the diagram that will not be used for analysis of the hollow sites' energy difference, namely, those taken at liquid nitrogen temperatures and a result obtained for the Cu(111)-$(6\sqrt{3}\times 6\sqrt{3})$R30°-Cl structure. These results are briefly discussed below.

Two distinctly different results were obtained for the $\theta = 0.33$ surface depending on whether the chlorine was introduced before or after the crystal was cooled to 190 K. In both cases, LEED showed a well-defined $\sqrt{3}$ structure and EDCs indicated identical surface concentration of chlorine, however $P_{(1-11)}$ values of 0.92 ± 0.02 for room temperature dosing and 0.83 ± 0.02 for low temperature dosing show that the distribution of chlorine atoms was remarkably different in either case. Following dosing at low temperature, the distribution of atoms between the two hollow sites is relatively even with $f_{\mathrm{hcp}} = 0.43 \pm 0.04$, whereas dosing at room temperature followed by cooling gave $f_{\mathrm{hcp}} = 0.19 \pm 0.08$, which is similar to results obtained at room temperature without cooling. These results demonstrate that on the timescale of the experiment (about two hours) equilibrium is not attained and furthermore appear to indicate that, following low temperature adsorption at least, metastable domains of $\sqrt{3}$ structure in hcp hollow sites are formed. If these do not form, the fraction of atoms contributing to the ordered regions would be less than 0.14 (compared to 0.62 for room temperature dosing), since disordered regions should contain at least as many atoms in fcc sites as there are in hcp sites. It seems unlikely that the fractional order spots in LEED would be of similar intensity for both surfaces if there was such a large difference in the area fraction of ordered atoms.

The lowest $P_{(1-11)}$ value of 0.81 ± 0.02 was found for the Cu(111)−$(6\sqrt{3}\times 6\sqrt{3})$R30°-Cl structure. This corresponds to an almost equal distribution of atoms between the two hollow sites, $f_{\mathrm{hcp}} = 0.47 \pm 0.04$. As indicated in Fig. 3, the coherent fraction for this surface was also very low, $F_{(1-11)} = 0.17 \pm 0.06$. The hexagonal compression layer model of Goddard and Lambert[15] should produce a coherent fraction of zero in NIXSW, whereas the domain-wall model, described by Andryuschechkin *et al.*[16] and convincingly supported with scanning tuneling microscopy data, would be expected to produce results with a higher coherent fraction (similar to the disordered surfaces described later), unless, as suggested in their paper, there is a significant relaxation of the domain walls. We note here that if the atoms were displaced only between hollow and bridge sites, we would expect the coherent fraction to be ~0.23 (which corresponds to all atoms located on bridge sites and reductions in coherent fraction, due to disorder, of a similar magnitude to the other surfaces studied here). This result does not help distinguish between either model, at best it signifies an avoidance of the atop site, which is unsurprising given that recent density functional theory (DFT) calculations[17] indicate an energy difference of ~420 meV between atop and hollow sites (compared to ~75 meV between bridge and hollow sites), however the determination of lateral interaction energies described later sheds a little more light on this issue.

MONTE CARLO SIMULATIONS IN COMPARISON TO NIXSW DATA

The disorder temperatures of both the $(\sqrt{3}\times\sqrt{3})$R30° and (2×2) structures were found by setting the coverage identical to the nominal coverage of these surfaces (0.33 and 0.25, respectively) and performing simulations at a variety of temperatures. The disorder temperature used in the foregoing was taken as the temperature at which $f_{\mathrm{hcp}} = 0.25$. Convergence was checked by running extended simulations at these temperatures to ensure that the fractional population did not irreversibly deviate from this value. Repeat simulations, both with smaller lattices and different initial positions of the random number generator, indicate that the error in these values is of the order of 1%. We find that the $(\sqrt{3}\times\sqrt{3})$R30° disorder temperature scales almost linearly with a sum of the interaction energies, as shown in Fig. 5. The sum is simply the

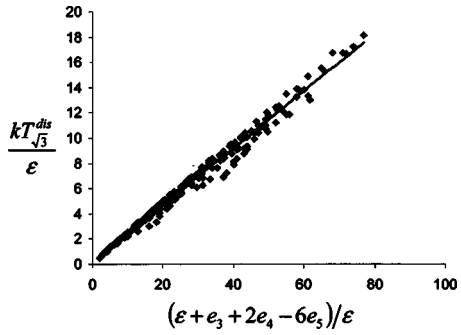

FIG. 5. Comparison of the disorder temperature of the Cu(111)-($\sqrt{3}\times\sqrt{3}$)R30°-Cl structure from Monte Carlo simulations and a linear sum of interaction energies representing the energy required to displace an atom from an ordered position.

energy difference between a fcc site in an ordered ($\sqrt{3}\times\sqrt{3}$)R30° structure and the neighboring hcp site and a linear fit leads to the empirical relationship given in Eq. (6).

$$kT_{\sqrt{3}}^{\mathrm{dis}} = 0.226(1.16\varepsilon + e_3 + 2e_4 - 6e_5). \tag{6}$$

A simple relationship of this kind is not so apparent for the (2×2) disorder temperature, although there appears to be an empirical correlation with the parameter given in the graph shown in Fig. 6, leading to the relationship in Eq. (7). There is no physical basis for this relationship [as is also true for Eq.(6)], however, it can be used to obtain an approximation of the (2×2) disorder temperature and notably, this temperature depends minimally, if at all, on the value of e_3.

$$kT_2^{\mathrm{dis}} = 0.247\left(1.38\varepsilon + 2e_4 + \frac{e_4e_5}{5\varepsilon}\right). \tag{7}$$

While there is some scatter in the latter of these graphs, the relationships provide an important starting point for the modeling of the Cu(111)-Cl system. Since the ($\sqrt{3}\times\sqrt{3}$)R30° disorder temperature is above room temperature and the (2×2) structure has never been observed even at

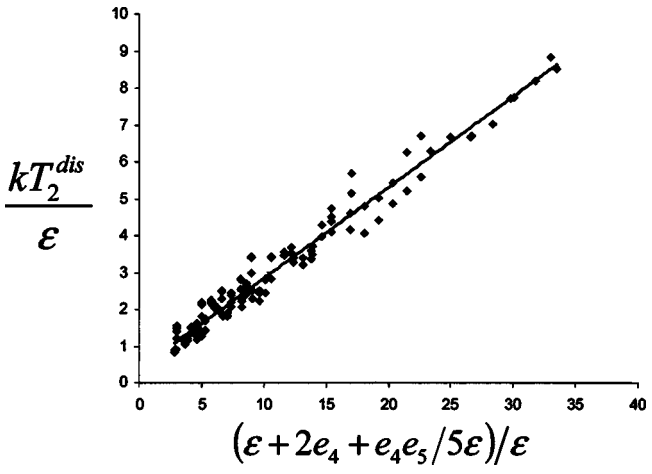

FIG. 6. Comparison of the disorder temperature of the Cu(111)-(2×2)-Cl structure from Monte Carlo simulations and a sum of interaction energies chosen to achieve as close to a linear relationship as possible.

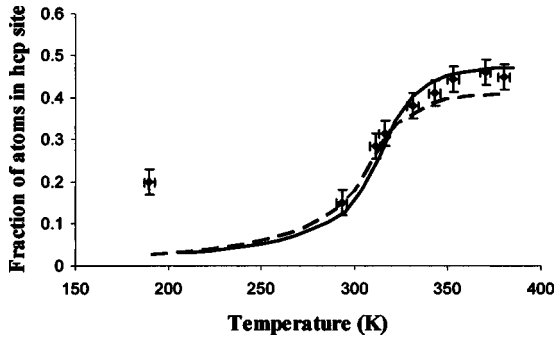

FIG. 7. Overlay of NIXSW data (points) of the Cu(111)-($\sqrt{3}\times\sqrt{3}$)R30°-Cl disorder transition with two Monte Carlo simulations with $e_3=20\varepsilon$ (solid line) and $e_3=4\varepsilon$ (dashed line). In both cases $e_4=e_3/2$ and $e_5=0$. The 189 K result is shown also, and is essentially identical to the room temperature result.

low temperatures, Eqs. (6) and (7) imply that either e_3 is large with respect to both ε and e_4, or that e_5 is negative and therefore an attractive potential. A strong attractive interaction at e_5 would suggest that at low temperatures islands of ($\sqrt{3}\times\sqrt{3}$)R30° structure will form well below the nominal one third coverage, which has not been observed experimentally. This expectation is confirmed by Monte Carlo simulations. We therefore included only weak attractive and repulsive interactions (of the order of ε) for e_5 in our simulations.

NIXSW results at a variety of temperatures with one third coverage of chlorine are plotted in Fig. 7 along with the results of two Monte Carlo simulations. There is no evidence in the experimental results, or in most of the simulations, of a discontinuous transition. We find that a large number of the simulations fit the curve within the error of the data, and as a result, this data is not very useful in the determination of ε. The only usable part of the data is in the completely disordered, high temperature surfaces for which $f_{\mathrm{hcp}}=0.45\pm0.03$. Simulations in which $e_3<5\varepsilon$ give poor agreement in this region, as shown by the curve for which $e_3=4\varepsilon$.

Disordered surfaces with low chlorine coverage were analysed by NIXSW and the results are shown in Fig. 8. All surfaces in this regime gave similar values for f_{hcp} ($\sim$0.45). Tellingly, the surfaces examined at quarter monolayer coverage were similar to lower coverage surfaces in the distribution of chlorine atoms between the two sites. Monte Carlo simulations demonstrate that at this coverage the range of interaction energies which match the data is somewhat limited, a representative sample of simulations is also plotted in Fig. 8. Interestingly, the simulations which best match the data have values of ε which can be estimated from the two level partition function of Eq. (1) with an error of less than 1 meV. This can be visualised in Fig. 8 by extrapolating the simulation data to zero coverage, when Eq. (1) becomes valid (since there are no lateral interactions in this limit). This approach would indicate that $\varepsilon=5$ meV, although the assumptions made in this calculation would not warrant reliance on this figure.

The result for quarter monolayer coverage at room temperature is the best indicator within our dataset of the value of ε. The dependence of f_{hcp} on the e_3, e_4, and e_5 parameters was determined at 293 K (room temperature, calibrated to

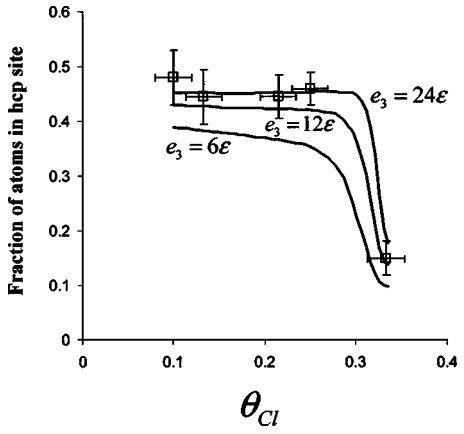

FIG. 8. Overlay of NIXSW data (points) taken at room temperature with different coverages of chlorine on Cu(111) and three Monte Carlo simulations with $e_4=2\varepsilon$ and $e_5=0$. The simulation with $e_3=24\varepsilon$ gives the best fit to the data.

the $(\sqrt{3}\times\sqrt{3})$R30° disorder temperature, which was independently determined for each set of parameters) and quarter monolayer coverage. Figure 9(a) shows how the fractional occupation of hcp sites changes for fixed values of $e_4=2\varepsilon$ and $e_5=0$ as the remaining parameter (e_3) is altered. The limiting value of $f_{\mathrm{hcp}}=0.42$ can be found by linear extrapolation between data points and is $e_3=13\varepsilon$. In Fig. 9(b) the effect of varying both e_3 and e_4 is shown with solid contour lines representing both the limiting and two other values of the fractional occupation of hcp sites. There is no substantive change in the diagram if e_5 is altered to $\pm\varepsilon$. However if it raised to 2ε or above, there is an increased stability of the (2×2) phase and if it is lowered to below 2ε, condensation of the $(\sqrt{3}\times\sqrt{3})$R30° phase starts to occur. Both of these situations have the effect of decreasing the fractional occupation of hcp sites and as a result e_3 and e_4 have to become significantly larger to satisfy the requirement of the NIXSW data. Since adequate fits to the data can be achieved with $e_5=0$, and for reasons given previously, we did not investigate the effect of varying e_5 to any greater extent than this.

Also shown in Fig. 9(b) are dashed contour lines representing the value of ε. These values can be directly determined from the disorder temperature of the $(\sqrt{3}\times\sqrt{3})$R30° phase in the simulations. It can be seen that, for the parameters we have simulated, ε must be less than 10 meV, and is more probably less than 5 meV. If it is 5 meV, as suggested earlier, and as indicated by DFT calculations,[17] then we find the most likely values for e_3 and e_4 to be ~105 and ~7 meV, respectively. This suggests that the lateral interaction between chlorine atoms is essentially hard walled, with very weak long range interactions. It is interesting to note that with these values of e_3 and e_4 the (2×2) disorder transition would be expected to occur at approximately 70 K (see Figs. 5 and 6), although the kinetics of ordering may be too slow at such temperatures to permit observation of this structure.

In all of the cases we have modeled, the e_3 interaction is of similar magnitude to the DFT calculated energy difference between the hollow and bridge sites (~75 meV).[17] This is interesting, as it would strongly indicate that the interaction

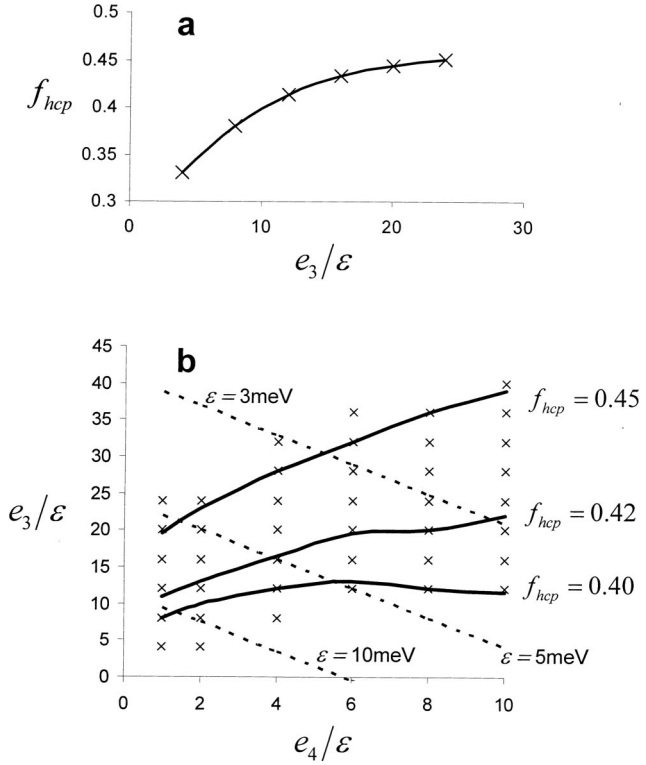

FIG. 9. Monte Carlo simulations carried out at room temperature and quarter monolayer coverage with $e_5=0$. (a) Fractional occupation of the hcp site increases as the e_3 interaction energy is increased, example shown is for $e_4=2\varepsilon$ (c.f. Fig. 8). (b) Contour plot of fractional occupation of the hcp site as both e_3 and e_4 are varied. Crosses indicate the simulations which were performed and solid contours representing f_{hcp} values of 0.40, 0.42 (the lower limit from the error in NIXSW analysis) and 0.45 (the NIXSW result) are plotted. The dashed lines represent contours of the value of ε, taken from the Cu(111)-$(\sqrt{3}\times\sqrt{3})$R30°-Cl disorder transition temperature, and are from the lower to upper contour 10, 5, and 3 meV, respectively.

energy corresponding to e_3 is substantially greater than we have reported and this interaction in the simulations actually models a displacement from a hollow to a bridge site rather than a movement between hollow sites. In comparison to the DFT calculated energy difference between atop and hollow binding (~420 meV) the e_3 interaction is somewhat weaker. This comparison is suggestive that the Cu(111)$-(6\sqrt{3}\times6\sqrt{3})$R30°-Cl structure is closer to the domain-wall model of Andryuschechkin *et al.*[16] with strong relaxation at the domain wall rather than the hexagonal compression layer model of Goddard and Lambert.[15] The e_3 interaction does not appear to be sufficiently large to promote atoms to the vicinity of the atop site which is an essential feature of the Goddard and Lambert model.

V. CONCLUSIONS

NIXSW data taken for a wide range of different coverages and temperatures of chlorine on Cu(111) are consistent with chlorine atoms only occupying hollow sites. In all cases, the

fractional occupation of the fcc hollow was greater than that of the hcp hollow demonstrating that this is the lowest energy site. Adsorption of chlorine at 190 K to one third monolayer coverage results in a different surface from that obtained by adsorption at room temperature followed by cooling, demonstrating that equilibration at this temperature is extremely slow. We report, for the first time, a NIXSW investigation of the $Cu(111)-(6\sqrt{3}\times 6\sqrt{3})R30°$-Cl and argue, on the basis of a comparison of the interaction energies determined in this work and the site energies calculated by Doll and Harrison,[17] that the domain wall model of Andryushechkin *et al.*[16] is consistent with our data.

Comparison of the NIXSW results with Monte Carlo simulations indicates that the energy difference between the two hollow sites is approximately 5 meV, and certainly less than 10 meV. This is in excellent agreement with DFT calculations but somewhat different to a previous investigation. Results can be adequately modelled with short range interactions which correlate well with the van der Waal's diameter of chlorine.

ACKNOWLEDGMENTS

The authors would like to thank CLRC Daresbury Laboratory for a Direct Access Award. We would also like to express gratitude, for advice and useful discussions from Nicholas Harrison and Klaus Doll, and to George Miller for his technical assistance on the beamline.

*Corresponding author: email address a.g.shard@sheffield.ac.uk

[1] J. Zegenhagen, Surf. Sci. Rep. **18**, 199 (1993); D. P. Woodruff, Prog. Surf. Sci. **57**, 1 (1998).
[2] C. Schwennicke, C. Voges, and H. Pfnur, Surf. Sci. **349**, 185 (1996).
[3] C. Schwennicke and H. Pfnur, Surf. Sci. **369**, 248 (1996).
[4] C. Schwennicke and H. Pfnur, Phys. Rev. B **56**, 10558 (1997).
[5] M. F. Kadodwala, A. A. Davis, G. Scragg, B. C. C. Cowie, M. Kerkar, D. P. Woodruff, and R. G. Jones, Surf. Sci. **324**, 122 (1995).
[6] D. P. Woodruff, B. C. C. Cowie, and A. R. H. F. Ettema, J. Phys.: Condens. Matter **6**, 10633 (1994).
[7] D. P. Woodruff, D. L. Seymour, C. F. McConville, C. E. Riley, M. D. Crapper, N. P. Prince, and R. G. Jones, Phys. Rev. Lett. **58**, 1460 (1987).
[8] A. W. Robinson, S. D'Addato, V. R. Dhanak, P. Finetti, and G. Thornton, Rev. Sci. Instrum. **66**, 1762 (1995).
[9] N. D. Spencer, P. J. Goddard, P. W. Davis, M. Kitson, and R. M. Lambert, J. Vac. Sci. Technol. A **7**, 1554 (1989).
[10] V. R. Dhanak, A. G. Shard, B. C. C. Cowie, and A. Santoni, Surf. Sci. **410**, 321 (1998).
[11] A. G. Shard and B. C. C. Cowie, J. Phys.: Condens. Matter **10**, L69 (1998).
[12] N. Metropolis, A. W. Rosenbluth, M. N. Rosenbluth, A. H. Teller, and E. Teller, J. Chem. Phys. **21**, 6 (1953).
[13] Makoto Matsumoto, Takuji Nishimura, http://www.math.keio.ac.jp (c)1997.
[14] M. D. Crapper, C. E. Riley, P. J. J. Sweeney, C. F. McConville, D. P. Woodruff, and R. G. Jones, Surf. Sci. **182**, 213 (1987).
[15] P. J. Goddard and R. M. Lambert, Surf. Sci. **67**, 180 (1977).
[16] B. V. Andryuschechkin, K. N. Eltsov, and V. M. Shevlyuga, Surf. Sci. **470**, L63 (2000).
[17] K. Doll and N. M. Harrison, Chem. Phys. Lett. **317**, 282 (2000).